

Charge-density-wave gap in the quasi-two-dimensional conductor $\text{Na}_{0.9}\text{Mo}_6\text{O}_{17}$ measured by angle-resolved photoemission spectroscopy

P.-A. Glans, T. Learmonth, and K. E. Smith*

Department of Physics, Boston University, 590 Commonwealth Avenue, Boston, Massachusetts 02215, USA

T. Valla and P. D. Johnson

Department of Physics, Brookhaven National Laboratory, Upton, New York 11973, USA

S. L. Hulbert

National Synchrotron Light Source, Brookhaven National Laboratory, Upton, New York 11973, USA

W. McCarroll and M. Greenblatt

Department of Chemistry, Rutgers University, New Brunswick, New Jersey 08903, USA

(Received 9 January 2005; published 14 July 2005)

The charge-density-wave gap in the quasi-two-dimensional conductor $\text{Na}_{0.9}\text{Mo}_6\text{O}_{17}$ has been measured using angle-resolved photoemission spectroscopy. The gap opening is accompanied by the creation of a new zone boundary and a subsequent backfold of the bands. The position of the point of minimum binding energy of the band dispersion has been determined in both energy and momentum. A change of the momentum of this point at very low temperatures is consistent with the existence of a second phase transition, previously observed by magnetic susceptibility and specific heat measurements. Symmetry arguments are used to show that the features found in the electronic structure are best described by using the monoclinic nomenclature, even though the measured low-energy electron diffraction patterns are hexagonal.

DOI: [10.1103/PhysRevB.72.035115](https://doi.org/10.1103/PhysRevB.72.035115)

PACS number(s): 79.60.-i

INTRODUCTION

The electronic properties of quasi-low-dimensional materials have been the focus of enduring scientific interest.^{1,2} Such materials often exhibit charge-density waves (CDWs) and periodic lattice distortions (PLDs). The CDW wave vector \mathbf{q} can be determined by the Fermi surface and can be either commensurate or incommensurate with the underlying lattice. When the CDW forms (at a temperature of T_{CDW}), the nested portions of the Fermi surface are destroyed and a gap opens up in the electronic density of states. Depending on how much of the Fermi surface is destroyed, the CDW can lead to either a metal-to-semiconductor transition or a metal-to-metal transition. These effects are generally associated with quasi-one-dimensional (1D) materials. In order to explain the existence of charge CDWs, PLDs, and Peierls transitions in both organic and inorganic quasi-*two*-dimensional (2D) conductors, the concept of hidden Fermi surface nesting was introduced by Whangbo *et al.*^{3,4} In this model, the real 2D Fermi surface is viewed as a combination of *quasi-1D* structures, with distinct 1D nesting vectors.^{3,4} Indirect experimental confirmation of this model came from x-ray diffraction measurements, which showed that the displacement vector of the structural instability in the quasi-2D conductors $\text{K}_{0.9}\text{Mo}_6\text{O}_{17}$ and $\text{Na}_{0.9}\text{Mo}_6\text{O}_{17}$ are consistent with the predicted “hidden” quasi-1D nesting wave vector.³ The first direct verification of the veracity of this model was obtained in a moderate resolution angle-resolved photoelectron spectroscopy (ARPES) study of $\text{Na}_{0.9}\text{Mo}_6\text{O}_{17}$.⁵

The CDW transition temperatures for $\text{K}_{0.9}\text{Mo}_6\text{O}_{17}$ and $\text{Na}_{0.9}\text{Mo}_6\text{O}_{17}$ are $T_{\text{CDW}}=120$ and 80 K, respectively.¹ Both

materials exhibit a metal-to-metal transition as confirmed by resistivity measurements.¹ While the crystal structure of $\text{K}_{0.9}\text{Mo}_6\text{O}_{17}$ is hexagonal,⁶ the structure of $\text{Na}_{0.9}\text{Mo}_6\text{O}_{17}$ is monoclinic pseudohexagonal.⁷ Due to the similarities in crystal structure, calculations of the electronic structure of $\text{KMo}_6\text{O}_{17}$ have been used to understand the properties of $\text{Na}_{0.9}\text{Mo}_6\text{O}_{17}$.^{3,8} Experimental results for $T > T_{\text{CDW}}$ indicate mixed results for this assumption.^{5,9} The data presented by Breuer *et al.* allowed for mirror operations along the X and Y directions in the Brillouin zone and translations by hexagonal lattice vectors, which lead to two 1D Fermi surfaces being reported.⁵ Gweon *et al.* assumed a hexagonal symmetry and the full Fermi surface map was created by 120° rotations; they reported three 1D Fermi surfaces.⁹ Thus while experimental data supports calculations of the electronic structure of $\text{K}_{0.9}\text{Mo}_6\text{O}_{17}$, there remains some uncertainty in the applicability of these calculations for $\text{Na}_{0.9}\text{Mo}_6\text{O}_{17}$.

We present here results of a new high-resolution ARPES study of the electronic structure near the Fermi level (E_F) of single-crystal $\text{Na}_{0.9}\text{Mo}_6\text{O}_{17}$. Measurements were made at temperatures between 23 and 200 K, above and below T_{CDW} . Our data reveal the existence of two closely spaced bands that disperse parallel to each other along most of the ΓM direction in the bulk Brillouin zone. The two bands remain separated as they cross E_F , leading to two discrete Fermi wave vectors (k_F) for $T > T_{\text{CDW}}$. We also observe the opening of a band gap at E_F for $T < T_{\text{CDW}}$ at specific parts of the Brillouin zone, as well as backfolding of the bands due to creation of a new zone boundary. Finally, while we are able to fully determine the size and location in the zone of the gap in one symmetry direction, we did not observe the gap in a hexagonally equivalent position in the zone.

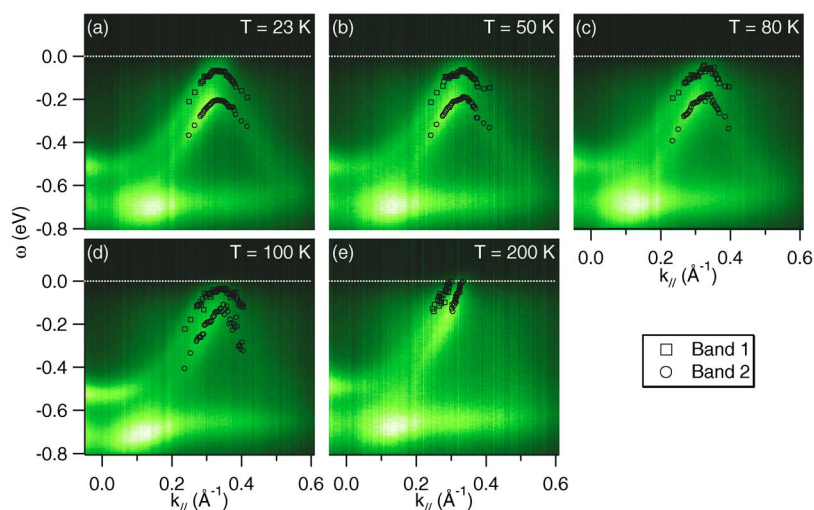


FIG. 1. (Color online) Intensity maps collected in the ΓM direction. (a)–(e) are for 23, 50, 80, 100, and 200 K, respectively. The position of the maximum intensity for each band is marked by squares for band 1 and circles for band 2. The positions were extracted by fitting two Lorentzians to EDCs.

EXPERIMENT

The experiment was performed at the normal incidence monochromator beamline U13UB at the National Synchrotron Light Source at Brookhaven National Laboratory. The spectra were taken using a Scienta SES-200 spectrometer. The spectrometer is mounted at a fixed angle of 45° to the incoming photon beam and the emission angle was varied by rotating the sample. Total energy resolution was set to better than 15 meV, as measured from the Fermi edge of Sr_2RuO_4 kept at ~ 5 K. The instrument has an angular resolution of better than $\pm 0.1^\circ$, which corresponds to a momentum resolution of $\pm 0.0038 \text{ \AA}^{-1}$ (equivalent to 0.6% of the ΓM distance in the bulk Brillouin zone of $\text{Na}_{0.9}\text{Mo}_6\text{O}_{17}$) for k_{\parallel} at the selected photon energy. Single crystals of $\text{Na}_{0.9}\text{Mo}_6\text{O}_{17}$ were grown by a temperature gradient flux technique. The samples were mounted on a liquid He cryostat, and cleaved *in situ* at liquid He temperatures in an ultrahigh vacuum chamber with a base pressure of better than 1×10^{-10} Torr. The temperature was controlled by a Lakeshore temperature controller and a calibrated silicon sensor mounted on the cryostat. Orientation of the crystal was checked by low-energy electron diffraction (LEED) after the photoemission experiment because the $\text{Na}_{0.9}\text{Mo}_6\text{O}_{17}$ surface is very sensitive to electron irradiation. The LEED pattern showed pinpoint sharp spots for about 10 s, after which time the spots became dim, indicating surface damage due to the electron beam. While the bulk crystal structure has been determined by x-ray diffraction to be monoclinic, the LEED patterns were observed to be hexagonal. We note that the crystal structure of $\text{Na}_{0.9}\text{Mo}_6\text{O}_{17}$ is very similar to that of $\text{K}_{0.9}\text{Mo}_6\text{O}_{17}$. $\text{Na}_{0.9}\text{Mo}_6\text{O}_{17}$ can be thought of as being hexagonal but with a slight distortion, making it monoclinic. We use the hexagonal labeling scheme in this paper for the following reasons. First, we could not distinguish experimentally between the ΓL and ΓZ directions in the ARPES spectra, both coinciding with the ΓM direction in the hexagonal Brillouin zone. This will be discussed further below. Second, the locations in k

space of the L and M points relative to the Γ point are almost identical, as is the distance between the Z point and the midpoint between Γ and M . Finally, the measured LEED pattern is clearly hexagonal.

RESULTS AND DISCUSSION

Figure 1 presents photoemission intensity maps recorded in the ΓM direction at the indicated temperatures, above and below the CDW transition temperature of 80 K. At all temperatures, three bands are clearly visible. Two of these bands disperse parallel to each other towards E_F with maximum binding energy at the zone center Γ . We designate these as bands 1 and 2, with band 1 lying closest to E_F at all values of k_{\parallel} . The third band is much less dispersive and is observed at a binding energy of approximately 0.8 eV at all sample temperatures; this band is designated as band 3. At 200 K, bands 1 and 2 are observed to cross E_F in the vicinity of $k_{\parallel} = 0.35 \text{ \AA}^{-1}$ [see Fig. 1(e)]. For temperatures ≤ 100 K [Figs. 1(a)–1(d)], the two bands do not cross E_F , but reach a minimum binding energy and disperse away from E_F to higher binding energies as k_{\parallel} is increased above 0.35 \AA^{-1} , indicating the creation of a new zone boundary at this point. The dispersion of the bands is indicated on each of the panels in Fig. 1, where the positions of the peaks were determined by fitting the energy distribution curves (EDCs) to Lorentzian line shapes. Note that even though the centroids of the dispersive bands do not cross E_F for $T \leq 100$ K, the leading edge of band 1 does reach E_F , and consequently there is some emission intensity at E_F . For this reason, energy gaps reported in this paper are the energy difference between E_F and the point of maximum intensity of a band at a particular k_{\parallel} . The measured bands agree in general with those from published tight-binding calculations.⁸ These calculations show that the bands are primarily derived from the t_{2g} block of Mo $3d$ states located on innermost two sublayers of the Mo_6O_{17} layer. The measured bandwidth is approximately twice that calculated;

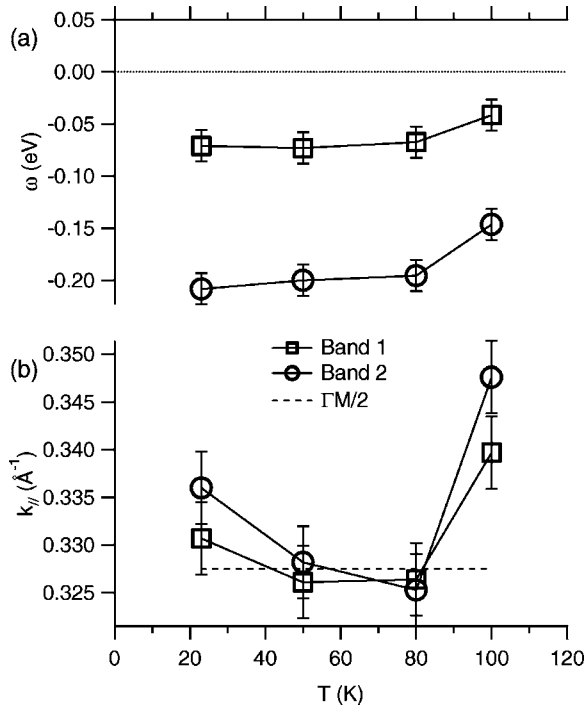


FIG. 2. (a) Magnitude of the energy gaps for bands 1 and 2 as a function of sample temperature. (b) Position in k space of the points of minimum binding energy for bands 1 and 2 as a function of the sample temperature. See text for details.

underestimation of bandwidths is a known issue for tight-binding calculations.

Figure 2(a) plots the minimum binding energy of bands 1 and 2 as a function of sample temperature ≤ 100 K. Figure 2(b) plots the value of k_{\parallel} for which the minimum binding energy occurs for both bands, also as a function of sample temperature. (As shown in Fig. 1, for 200 K, both bands 1 and 2 cross E_F , so at that temperature the minimum binding energy of these bands is zero.) As the temperature is reduced, changes in the minimum binding energy for both bands can be observed in Fig. 2(a). Band 2 shows the greater shift in energy. The minimum binding energy for band 2 changes from 0.15 eV at $T=100$ K to 0.20 eV at $T=23$ K (below T_{CDW}), while the minimum binding energy for band 1 changes from 0.04 eV at $T=100$ K to 0.07 eV below T_{CDW} . The position along ΓM where the bands make their closest approach to E_F also varies as the temperature is reduced. At 100 K, above T_{CDW} , the points of minimum binding energy for both bands occur well past half the distance between Γ and M ($\Gamma M/2=0.3275 \text{\AA}^{-1}$). For 80 and 50 K, the points of minimum binding energy are at $\Gamma M/2$, but at 23 K the points of minimum binding energy again shift to $>\Gamma M/2$. In contrast, the energy gap for bands 1 and 2 does not behave anomalously at 23 K (Fig. 2(a)).

At 200 K both bands 1 and 2 cross E_F at Fermi wave vectors of $k_{F1}=0.304 \text{\AA}^{-1}$ and $k_{F2}=0.334 \text{\AA}^{-1}$. These are less than and greater than $q_{CDW}/2$ (0.3275\AA^{-1}), respectively. At $T=100$ K, the point of minimum binding energy of band 2 is at 0.345\AA^{-1} (53.1% of ΓM), while the point minimum binding energy of band 1 is at 0.340\AA^{-1} (51.9% of ΓM). As the temperature decreases through 50 K, the points of minimum

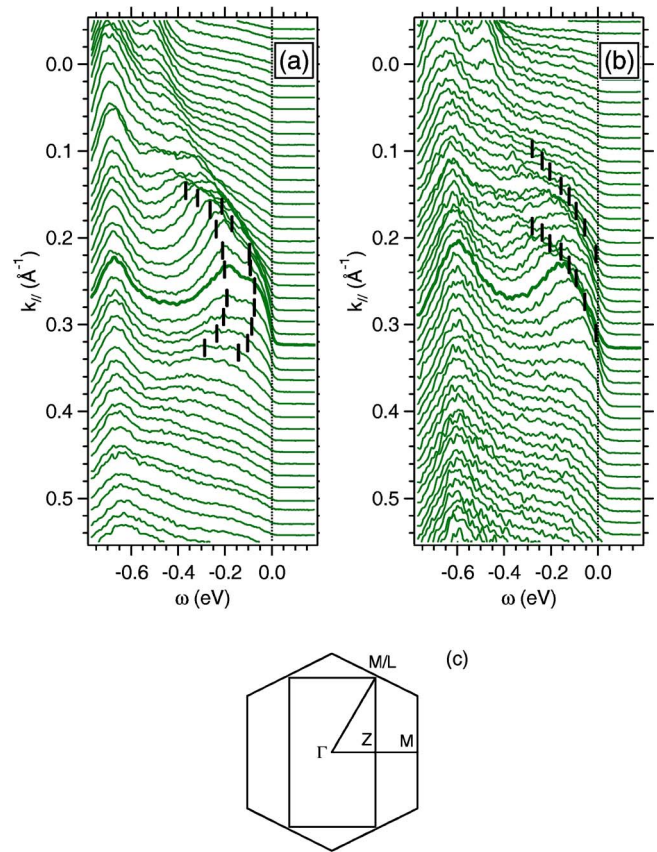


FIG. 3. (Color online) A comparison between two sets of EDCs, both recorded in the ΓM direction (as determined by LEED). Both sets were recorded with the sample at approximately 50 K. The EDCs in (a) are the same data as in Fig. 1(b). (c) shows the hexagonal Brillouin zone for $\text{KMo}_6\text{O}_{17}$, which is almost isostructural with $\text{Na}_{0.9}\text{Mo}_6\text{O}_{17}$. In (a) there is a backfolded band and in (b) there is no backfolding and both bands cross E_F .

binding energy of both bands lie at the same place in k space and also coincide, as expected, with q_{CDW} . [The nesting vectors for $\text{K}_{0.9}\text{Mo}_6\text{O}_{17}$ have been shown to be $q_a=(a^*/2, 0, 0)$, $q_b=(0, b^*/2, 0)$, and $q_{a+b}=(a^*/2, b^*/2, 0)$.¹⁰ Since the crystal structure of $\text{Na}_{0.9}\text{Mo}_6\text{O}_{17}$ is very similar, we expect a similar $q_{CDW}=0.655 \text{\AA}^{-1}$.] However, as the temperature is decreased to 23 K, k_{\parallel} for the point of minimum binding energy of the bands increases. We note that a second transition has been observed by magnetic susceptibility and specific heat measurements in the vicinity of 30 K.¹ The origin of this transition is not known, although there has been speculation that it could be driven by a spin-density wave (SDW). The change we observe for the point of minimum binding energy k_{\parallel} is quite small, from 50.0% to 50.9% of ΓM when going from $T=50$ K to $T=23$ K. While the CDW is commensurate below T_{CDW} , (with the possible exception of at the lowest temperatures), we do have evidence of a noncommensurate precursor state at $T=100$ K, above T_{CDW} . This is seen in Fig. 1(d), where a point of minimum binding energy can be observed for both bands, and neither band crosses E_F . A sliding incommensurate CDW can give rise to nonlinear transport properties. However, a sliding incommensurate CDW has not been observed, either because the deviation from commensurate is very small or the CDW is pinned.

If the surface Brillouin zone is hexagonal, the same electronic structure should be measured along every ΓM direction, since all are equivalent. “Figures 3(a) and 3(b) present two sets of EDCs for data taken at $T \approx 50$ K, for states along what should be two equivalent ΓM directions, based on the LEED pattern. In Fig. 3(c) the hexagonal and the monoclinic Brillouin zones are included to show how the respective zones relate to each other. [The EDCs of Fig. 3(a) represent the same data as in Fig. 1(b)]. Clear differences are visible between the EDCs of Fig. 3(a) and Fig. 3(b). Specifically, the bands in Fig. 3(b) cross E_F and the bands in Fig. 3(a) do not. The EDCs in Fig. 3(b) were recorded at a temperature no higher than 50 K, well below the transition temperature. The markers in Fig. 3(a) are at the exact same positions as for the intensity map in Fig. 1(b). The markers in Fig. 3(b) are at the peak positions as determined by fitting to momentum distribution curves (MDCs). When recording the data for Fig. 3(b), data were taken from well into the second Brillouin zone (not shown). In the second zone the two bands are repeated as expected. The difference between k_{F1} and k_{F2} in the first and second zones is very small. From this one can conclude that the data in Fig. 3(b) are from the ΓM direction (or at least from a line slightly displaced from, but parallel to, the ΓM line). The difference between k_{F1} and k_{F2} in Fig. 1(e) is even smaller, so this measured direction is at least not displaced any further from ΓM than the data in Fig. 3(b), if at all. The theoretical calculations for $K_{0.9}Mo_6O_{17}$ predict the two Fermi-level crossings to be at their closest point to each other in the ΓM direction. This may indicate that we have two nonequivalent ΓM directions, at least in the CDW phase. A possible explanation would be that we have measured ΓM and $\Gamma M'$ directions. However, as we have previously reported, it is more probable that there are two plus four equivalent directions, as is suggested by the two overlaid zones presented in Fig. 3(c).⁵ Two ΓM directions coincide with ΓZ in the monoclinic zone scheme and four ΓM direc-

tions coincide with the monoclinic ΓL directions. A problem with assuming threefold rotational symmetry for q_{CDW} is that there is no reason for the wave vector to favor “positive” directions over “negative.” The measured effects of q_{CDW} (the gap, in this case) should show up with sixfold rotational symmetry. Since this is not observed, it is clear that the gap opens up within a “two plus four” symmetry.

CONCLUSION

We have found and characterized the CDW gap in the sodium purple bronze, $Na_{0.9}Mo_6O_{17}$. The gap opening is accompanied by the creation of a new zone boundary and a subsequent backfold of the bands. The position of the point of minimum binding energy in the band dispersion has been determined in both energy and momentum. A change of the momentum of the point of minimum binding energy at very low temperatures is consistent with the existence of a second phase transition, previously observed by magnetic susceptibility measurements and specific heat measurements. Symmetry arguments have been used to show that the features found in the electronic structure are best described by using the monoclinic nomenclature, even though the LEED patterns are hexagonal and evidence for the short periodicity (ΓZ) has not been found in the data.

ACKNOWLEDGMENTS

The Boston University program is supported in part by the Department of Energy under Grant No. DE-FG02-98ER45680. The BNL program was supported by the Department of Energy under Grant No. DE-AC02-98CH10886. Experiments were performed at the NSLS, which is supported by the Department of Energy, Divisions of Materials and Chemical Sciences.

*Corresponding author. Electronic mail: ksmith@bu.edu

¹M. Greenblatt, Chem. Rev. (Washington, D.C.) **88**, 31 (1988).

²K. E. Smith, Solid State Sci. **4**, 359 (2002); Annu. Rep. Prog. Chem., Sect. C: Phys. Chem. **90**, 115 (1995).

³M.-H. Whangbo, E. Canadell, P. Foury, and J.-P. Pouget, Science **252**, 96 (1991).

⁴M. H. Whangbo, J. Ren, W. Liang, E. Canadell, J. P. Pouget, S. Ravy, J. M. Williams, and M. A. Beno, Inorg. Chem. **31**, 4169 (1992).

⁵K. Breuer, C. B. Stagarescu, K. E. Smith, M. Greenblatt, and W. McCarroll, Phys. Rev. Lett. **76**, 3172 (1996).

⁶H. Vincent, M. Ghedira, J. Marcus, J. Mercier, and C. Schlenker, J. Solid State Chem. **47**, 113 (1983).

⁷B. M. Gatehouse, D. J. Lloyd, and B. K. Miskin, in *Proceedings*

of the 5th Materials Research Symposium—Solid State Chemistry, edited by R. S. Roth and S. J. Schneider, Nat. Bur. Stand. (U.S.) Spec. Publ. 364, 15 (1972); C. Schlenker, J. Dumas, C. Escribe-Filippini, H. Guyot, J. Marcus, and G. Fourcaudot, Philos. Mag. B **52**, 643 (1985).

⁸M. H. Whangbo, E. Canadell, and C. Schlenker, J. Am. Chem. Soc. **109**, 6308 (1987).

⁹G. H. Gweon, J. W. Allen, J. A. Clack, Y. X. Zhang, D. M. Poirier, P. J. Benning, C. G. Olson, J. Marcus, and C. Schlenker, Phys. Rev. B **55**, R13353 (1997).

¹⁰C. Escribe-Filippini, K. Konate, J. Marcus, C. Schlenker, R. Al-mairac, R. Ayroles, and C. Roucau, Philos. Mag. B **50**, 321 (1984).